

To Achieve Security and High Spectrum Efficiency: A New Transmission System Based on Faster-than-Nyquist and Deep Learning

Peiyang Song* and Fengkui Gong*

*State Key Laboratory of ISN, Xidian University, Xi'an, 710071, China

Email: pysong@stu.xidian.edu.cn, fkong@xidian.edu.cn

Abstract—With the rapid development of various services in wireless communications, spectrum resource has become increasingly valuable. Faster-than-Nyquist (FTN) signaling, which was proposed in the 1970s, has been a promising paradigm to improve the spectrum utilization. In this paper, we try to apply FTN into secure communications and propose a secure and high-spectrum-efficiency transmission system based on FTN and deep learning (DL). In the proposed system, the hopping symbol packing ratio with random values makes it difficult for the eavesdropper to obtain the accurate symbol rate and inter-symbol interference (ISI). While the receiver can use the blind estimation to choose the true parameters with the aid of DL. The results show that without the accurate symbol packing ratio, the eavesdropper will suffer from severe performance degradation. As a result, the system can achieve a secure transmission with a higher spectrum efficiency. Also, we propose a simplified symbol packing ratio estimation which has been employed in our proposed system. Results show that the proposed simplified estimation achieves nearly the same performance as the original structure while its complexity has been greatly reduced.

Index Terms—secure communications, faster-than-Nyquist signaling, blind estimation, deep learning, spectrum efficiency

I. INTRODUCTION

The last several decades have witnessed the rapid development of terrestrial wireless communications, including the widely concerned the fifth-generation mobile communications (5G), as well as the increasing demands for data traffic by various communication services. However, due to the limited coverage area and some economic reasons, there is still a large population that is excluded by the terrestrial communication networks. Inspired by this problem, in recent years, satellite communications have attracted more attention in both the academic and industrial fields for its wide coverage and the ability to provide seamless service for users located in some extreme areas (e.g. oceans, deserts and mountains).

FTN signaling was firstly proposed in the 1970s by *Bell Laboratories* and has been rediscovered and widely studied since the 2000s. It is promising to provide higher symbol rate and spectrum efficiency in future satellite communications (e.g. DVB-S2X [1]).

As known, in conventional Nyquist-criterion communications, the symbol duration must be set as $T > T_N = 1/(2W)$ to guarantee the performance of the transmission system, where W is the transmission bandwidth. In such scenarios, the receiver can effectively recover the transmitted symbols from

received ones benefiting from the strict orthogonality between different symbols. FTN signaling, in contrast, destroys the orthogonality and introduces unavoidable ISI by applying a smaller symbol duration $T < T_N$. This can obviously improve the transmission rate, yet as well as the complexity of the receiver to recover the transmitted symbols.

Fortunately, Mazo [2] has proved that the FTN signaling can improve as high as 25% transmission rate than the conventional Nyquist-criterion communication scheme in the additive white Gaussian noise (AWGN) channel with no loss of BER performance and any extra spectrum consuming, which is known as *the Mazo limit*.

Nowadays, a lot of researches have been conducted on signal detection for FTN signaling. And similar to conventional equalizers to eliminate the ISI from channels, the detection for FTN signaling contains time-domain and frequency-domain algorithms. Among time-domain detections, [3] and [4] employ the Viterbi algorithm where FTN signaling is considered as a special type of convolutional code. In [5], a very low-complexity symbol-by-symbol detection with near-optimal BER performance is developed. The combination of DL and FTN detection is studied in [6] where two DL-based FTN receiver designs are proposed. Meanwhile, there are also a number of papers focusing on the frequency-domain detections. Reference [7] applies the minimum mean square error (MMSE) criterion and proposes a frequency-domain equalizer for FTN signaling. Reference [8] further considers channel estimation and develops an iterative detection algorithm.

Due to the fact that the FTN signaling has several key parameters which can significantly affect the system performance, it is easy to think about the application of FTN into secure communications. Reference [9] has provided an attempt on this issue and proposed a safe transmission based on FTN with hopping filter roll-off factors. Under such a paradigm, the changing roll-off factor is known by both the transmitter and the receiver but is secret for the eavesdropper. However, as far as we know, the FTN with hopping symbol packing ratio, especially with random values which are known only by the transmitter, has not been studied yet.

Another important inspiration of this paper is the trend appeared recently to merge the DL with communications. So far, DL has been successfully employed in orthogonal frequency-division multiplexing (OFDM) [10], [11], cooperative communications with relay selection [12], device-to-

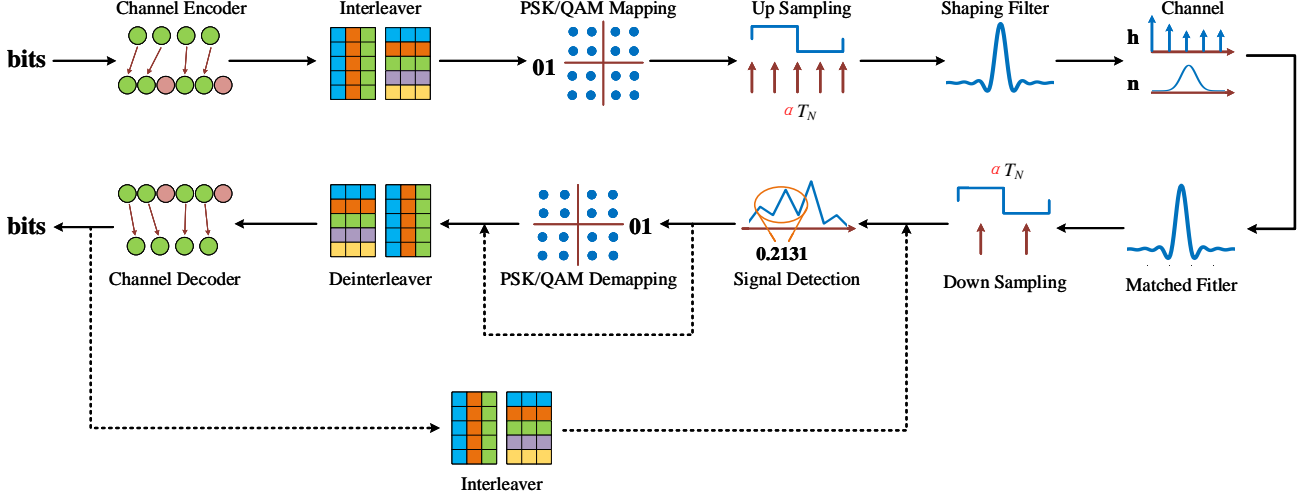


Fig. 1. System model of conventional FTN signaling

device (D2D) communications [13], etc. It is worth noting that, apart from the above mentioned reference [6], DL has also been employed in FTN for the blind symbol packing ratio estimation [14]. All these previous works inspire our study on the application of FTN into secure communications with the aid of DL.

The contribution of this paper can be summarized as follows.

- We propose an FTN-based secure and high-spectrum-efficiency transmission system with the aid of state-of-the-art DL technology, where the receiver only needs to know when the symbol packing ratio of the FTN transmitter changes, but not necessarily the accurate value.
- We propose a DL-based simplified symbol packing ratio estimation, which has been proved to perform nearly the same performance as the original architecture.
- We have carried out comprehensive evaluations to verify and analyze the security, performance and complexity of the proposed secure and high-spectrum-efficiency transmission system.

Herein, we give the definition of notations which we will encounter throughout the rest of the paper. Bold-face lower case letters (e.g. \mathbf{x}) are applied to denote column vectors. Light-face italic letters (e.g. x) denote scalers. x_i is the i -th element of vector \mathbf{x} . $x(t) * y(t)$ denotes the convolution operation between $x(t)$ and $y(t)$. $\lfloor x \rfloor$ is the maximum integer less than or equal to x . And $\|\mathbf{W}\|_0$ represents the number of non-zero items in matrix \mathbf{W} .

II. SYSTEM MODEL OF FTN

In this paper, we consider the complex-valued quadrature amplitude modulation (QAM) and AWGN channel. The conventional architecture of FTN signaling is illustrated as Fig. 1. In the transmitter, the signal that has passed through the shaping filter $h(t)$ can be written as

$$s(t) = \sqrt{P_s} \sum_{k=-\infty}^{+\infty} x_k h(t - k\alpha T_N), \quad (1)$$

where P_s is the average power of the bandwidth signals, x_k ($k = 0, \pm 1, \pm 2, \dots$) is the k -th symbol and α ($0 < \alpha \leq 1$) is called the symbol packing ratio which is applied to change the symbol duration. Due to the fact that the shaping filter function values 0 after every T_N , when $\alpha < 1$ is employed, the filtered symbols are no longer orthogonal and become the weighted sum of several successive symbols.

Corresponding to the shaping filter, a filter with a conjugate structure named matched filter is employed in the receiver to maximize the signal-to-noise ratio (SNR) of the received symbols. The filtered symbols can be written as

$$\begin{aligned} y(t) &= (s(t) + n(t)) * h(t) \\ &= \sqrt{E_s} \sum_{k=-\infty}^{+\infty} x_k g(t - k\alpha T_N) + \tilde{n}(t), \end{aligned} \quad (2)$$

where $g(t) = \int h(x)h(t-x)dx$, $\tilde{n}(t) = \int n(x)h(t-x)dx$, and $n(t)$ is the Gaussian white noise with power σ^2 .

Finally, the samples of the received symbols can be formulated as (3).

As seen, different from the conventional Nyquist-criterion transmission system, each sampled symbol in FTN signaling contains not only the expected symbol but also the adjacent ones. Meanwhile, due to the non-orthogonality between different samples in the matched filter, the noise in y_n becomes colored noise. All these new features make it more difficult to recover the original symbols in the FTN receiver.

$$\begin{aligned} y_n &= \sqrt{E_s} \sum_{k=-\infty}^{+\infty} x_k g(n\alpha T_N - k\alpha T_N) + \tilde{n}(n\alpha T_N) \\ &= \sqrt{E_s} \sum_{k=-\infty}^{n-1} x_k g((n-k)\alpha T_N) + \sqrt{E_s} x_n g(0) \\ &\quad + \sqrt{E_s} \sum_{k=n+1}^{+\infty} x_k g((n-k)\alpha T_N) + \tilde{n}(n\alpha T_N). \end{aligned} \quad (3)$$

III. THE PROPOSED SECURE TRANSMISSION SYSTEM WITH HIGH SPECTRUM EFFICIENCY

In this section, we provide the detailed introduction of the proposed safe and high-spectrum-efficiency transmission system. And following the general practice, we use Alice, Bob and Eve to represent the transmitter, the receiver and the eavesdropper.

A. System Architecture

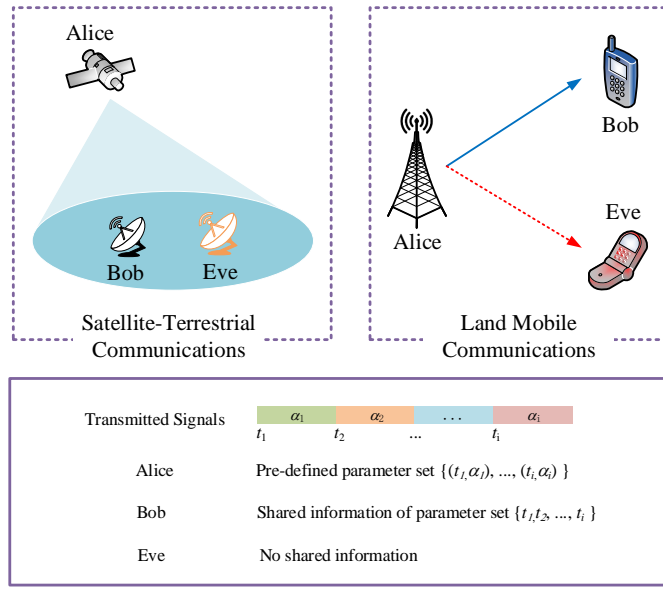


Fig. 2. Architecture of the proposed safe and high-spectrum-efficiency transmission system

As shown in Fig. 2, in the proposed FTN transmission system, the symbol packing ratio in the transmitter changes at every certain moment, which divides the transmitted symbols into different parts and results in different transmission rates in each part. Different from the conventional parameter-hopping safe transmissions (e.g. frequency-hopping communications), in the proposed system, Bob does not need to know exactly the time-value pair of the symbol packing ratio. The only necessary information is simply when the parameter changes. Then, the DL-based symbol packing ratio estimation will help Bob to get the true parameter value in time with the aid of the exact starting position.

However, for Eve, it may result in trouble to recover the transmitted symbols. For one thing, the change of the symbol packing ratio only affects the baseband symbols and can not be caught by analysis of the frequency spectrum. For another, the blind estimation suffers from the ambiguity between different parts and cannot indicate the accurate starting position. Once Eve employs a wrong symbol packing ratio, the sampled points will severely deviate from their correct positions, which makes it meaningless to further detect the signals and estimate the next symbol packing ratio.

B. A Simplified Symbol Packing Ratio Estimation for FTN Signaling

In this part, we propose a simplified symbol packing ratio estimation for FTN signaling. The complete architecture of the proposed estimation is shown in Fig. 3. When the received symbols have passed through the matched filter and be sampled, they are applied as the input of several analysis models. The main task of the analysis for α_k is to decide whether $\alpha_A = \alpha_k$, where α_A is the symbol packing ratio employed by Alice.

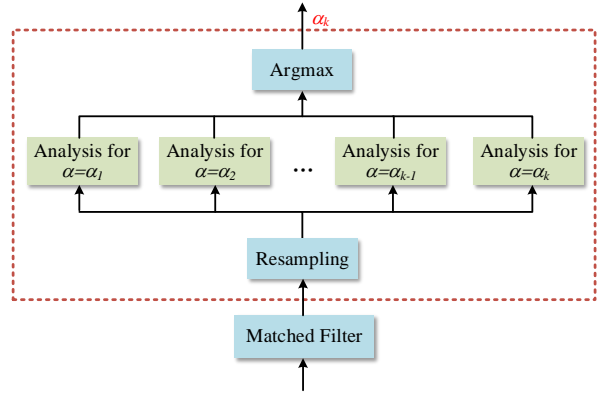


Fig. 3. Structure of the symbol packing ratio estimation employed in the proposed system

The detailed structure of the analysis for $\alpha = \alpha_k$ is shown in Fig. 4. Firstly, the input symbols are down-sampled by the shared starting position and interval $\alpha_i T_N$. Then, through serial-parallel conversion (S/P), the sampled serial symbols are reformed and fed into the deep neural network (DNN). After that, the output of the DNN, which can be regarded as the probability of $\alpha_A = \alpha_k$, will be transformed into 0 (false) or 1 (true). And finally, the count of true decisions during a certain time will be output.

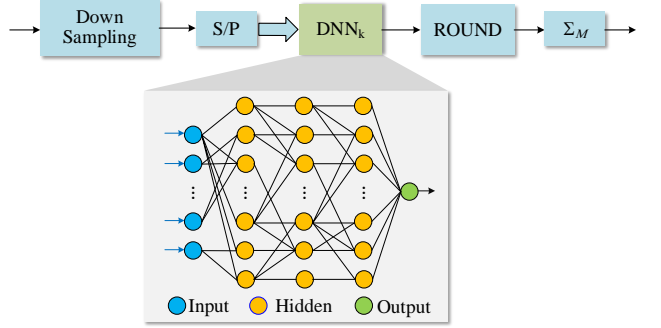


Fig. 4. Structure of the analysis for α_k in the proposed simplified symbol packing ratio estimation

The DNN we employed in Fig. 4 contains an input layer, three hidden layers and an output layer. Each hidden layer is essentially a sparsely connected layer with ReLU as its activation function. The system function of the DNN can be written as

$$\mathbf{y} = g_4(f(g_3(f(g_2(f(g_1(\mathbf{x}))))))), \quad (4)$$

where $f(\mathbf{x})_i = \max(x_i, 0)$ is the item-wise ReLU function to vector \mathbf{x} . $g_i(\mathbf{x}) = \mathbf{W}_i \mathbf{x} + \mathbf{b}_i$, where \mathbf{W}_i and \mathbf{b}_i are respectively the weight matrix and bias vector in the i -th layer of the DNN.

Benefiting from that the starting position of each employment of new α is shared by Alice, Bob does not need to divide the signal into several branches [14] to avoid the sampling offset. So, the multiplexer (MUX), the demultiplexer (DEMUX) and the decision parts in the original structure can be removed, which can reduce the complexity of the estimation to a certain degree.

Meanwhile, we focus on the simplification of the DNN, the main idea of which is to reduce the amounts of items in the weight matrices. Here, we employ an iterative strategy. After the model is well trained, we remove the items in \mathbf{W}_i which are near to 0 and then train the remaining network. Then, we iteratively carry out this process until the designed iteration counts or target sparsity ratio.

IV. AVERAGE SPECTRUM EFFICIENCY

A. Capacity of the Alice-Bob Link in AWGN Channel

For the Alice-Bob link, α can be easily obtained with the help of blind estimation and the exact starting position. So, α can be regarded as the shared information between Alice and Bob. And the transmission turns to be a conventional FTN signaling. The power of the transmitted signal can be written as

$$\sigma_s^2 = P_s \alpha T_N. \quad (5)$$

The capacity of FTN signaling can be formulated as [15]

$$R_B(\alpha) = \frac{1}{2\pi\alpha T_N} \int_0^\pi \log_2 \left(1 + \frac{2\sigma_s^2}{N_B} H(\alpha, \omega) \right) d\omega, \quad (6)$$

where $N_B/2$ is the power spectrum density of the Gaussian noise in the AWGN channel. And $H(\alpha, \omega)$ is defined as

$$H(\alpha, \omega) = \frac{1}{\alpha T_N} \sum_{k=-\infty}^{\infty} \left| G \left(\frac{\omega}{2\pi\alpha T_N} + \frac{k}{\alpha T_N} \right) \right|^2, \quad (7)$$

where $G(f)$ represents the Fourier transform of shaping filter function $h(t)$. Aided by the known system bandwidth which can be obtained by $W = 1/(2T_N) = W_T/(1+\beta)$, where W_T is the total bandwidth of the channel, the spectrum efficiency of the Alice-Bob link can be written as

$$C_B(\alpha) = \frac{1}{\pi\alpha(1+\beta)} \int_0^\pi \log_2 \left(1 + \frac{2\sigma_s^2}{N_B} H(\alpha, \omega) \right) d\omega. \quad (8)$$

Here, we define three bound function $b_1(\alpha) = \alpha\pi(1-\beta)$, $b_2(\alpha) = 2\pi - \alpha\pi(1+\beta)$ and $b_3(\alpha) = 2\pi - b_2(\alpha)$. According to the definition of the SRRC filter, for a certain combination of α and β , $H(\alpha, \omega)$ can be written as

$$H(\alpha, \omega) = \begin{cases} H_1(\alpha, \omega) & b_2(\alpha) < \pi \\ H_2(\alpha, \omega) & b_2(\alpha) \geq \pi \end{cases}, \quad (9)$$

where

$$H_1(\alpha, \omega) = \begin{cases} \frac{1}{\alpha}, & \omega \in [0, b_1(\alpha)) \\ \frac{1}{\alpha} G^2 \left(\frac{\omega}{2\pi\alpha T_N} \right), & \omega \in [b_1(\alpha), b_2(\alpha)) \\ \frac{1}{\alpha} \left(G^2 \left(\frac{\omega}{2\pi\alpha T_N} \right) + G^2 \left(\frac{\omega-2\pi}{2\pi\alpha T_N} \right) \right), & \omega \in [b_2(\alpha), \pi] \end{cases} \quad (10)$$

and

$$H_2(\alpha, \omega) = \begin{cases} \frac{1}{\alpha}, & \omega \in [0, b_1(\alpha)) \\ \frac{1}{\alpha} \left(G^2 \left(\frac{\omega}{2\pi\alpha T_N} \right) \right), & \omega \in [b_1(\alpha), b_3(\alpha)) \\ 0, & \omega \in [b_3(\alpha), \pi] \end{cases}. \quad (11)$$

Then, we split $C_B(\alpha)$ into several subsection integral and calculate them respectively. For $\omega \in [0, b_1(\alpha))$, the integral can be calculated as

$$C_{R1}(\alpha) = \int_0^{b_1(\alpha)} \log_2 \left(1 + \frac{2\sigma_s^2}{N_B} H(\alpha, \omega) \right) d\omega, \quad (12)$$

$$= \alpha\pi(1-\beta) \log_2 \left(1 + \frac{2\sigma_s^2}{\alpha N_B} \right)$$

According to the Gaussian-Chebyshev quadrature [16], for $\omega \in [b_1(\alpha), \pi]$, the integral can be written as

$$C_{R2}(\alpha) = \int_{b_1(\alpha)}^\pi \log_2 \left(1 + \frac{2\sigma_s^2}{N_B} H(\alpha, \omega) \right) d\omega \quad (13)$$

$$\approx C_1 \sum_{i=1}^N m_i \log_2 \left(1 + \frac{2\sigma_s^2}{N_B} H(\alpha, \omega_{1i}) \right),$$

where

$$C_1 = \frac{\pi [1 + \alpha(\beta - 1)]}{2}, \quad (14)$$

$$m_i = \frac{\pi \left| \sin \left(\frac{\pi(2i-1)}{2N} \right) \right|}{N} \quad (15)$$

and

$$\omega_{1i} = \frac{\pi}{2} \left\{ [1 + \alpha(\beta - 1)] \cos \left(\frac{\pi(2i-1)}{2N} \right) + 1 - \alpha(\beta - 1) \right\}. \quad (16)$$

Similarly, for $\omega \in [b_1(\alpha), b_3(\alpha))$, (8) can be written as

$$C_{R3}(\alpha) = \int_{b_1(\alpha)}^{b_3(\alpha)} \log_2 \left(1 + \frac{2\sigma_s^2}{N_B} H(\alpha, \omega) \right) d\omega \quad (17)$$

$$\approx C_2 \sum_{i=1}^N m_i \log_2 \left(1 + \frac{2\sigma_s^2}{N_B} H(\alpha, \omega_{2i}) \right),$$

where

$$C_2 = \pi\alpha\beta \quad (18)$$

and

$$\omega_{2i} = \pi\alpha \left(1 + \beta \cos \left(\frac{\pi(2i-1)}{2N} \right) \right). \quad (19)$$

Finally, the capacity of the proposed scheme in AWGN channel can be written as

$$C_{B'}(\alpha) = \begin{cases} C_{R1}(\alpha) + C_{R2}(\alpha), & b_2(\alpha) < \pi \\ C_{R1}(\alpha) + C_{R3}(\alpha), & b_2(\alpha) \geq \pi \end{cases}. \quad (20)$$

For the convenience of implementation, the set of available α values is usually a finite set in practical systems. Meanwhile, to avoid the possible detection and attack, every choice of α should be employed with the same probability. So, for the proposed transmission system, the average spectrum efficiency can be written as

$$C_{AB} = \frac{1}{N_\alpha} \sum_{i=1}^{N_\alpha} C_B(\alpha_i), \quad (21)$$

where α_i ($i = 1, 2, \dots, N_\alpha$) is the i -th symbol packing ratio that is employed in the transmission system.

B. Analysis of Alice-Bob Link in Rayleigh and Nakagami Channel

For the Rayleigh and Nakagami channel, the channel gain is taken into consideration and can be regarded as a constant during every data block in this paper. So, the power of the signal in the receiver with channel gain h can be written as

$$\sigma_{s'}^2(h) = h^2 P_s \alpha T_N. \quad (22)$$

The capacity of FTN signaling with certain channel gain h and packing ratio α can be obtained as

$$R_{B'}(\alpha) = \frac{1}{2\pi\alpha T_N} \int_0^\pi \log_2 \left(1 + \frac{2\sigma_{s'}^2(h)}{N_B} H(\alpha, \omega) \right) d\omega. \quad (23)$$

Considering that h is a random variable in Rayleigh and Nakagami channel, the mean capacity of the FTN signaling with packing ratio α can be formulated

$$C_{B'}(\alpha) = \frac{1}{\pi\alpha(1+\beta)} \cdot \underbrace{\int_0^\pi \int_0^{+\infty} f(h) \cdot \log_2 \left(1 + \frac{2h^2 P_s \alpha T_N}{N_B} H(\alpha, \omega) \right) dh d\omega}_{C_{i1}(\alpha, \omega)}, \quad (24)$$

where $f(h)$ is the probability density function (PDF) of the channel gain h . Here, we firstly consider the Rayleigh channel, where $f(h)$ can be written as

$$f(h) = f_R(h) = \frac{h}{\sigma^2} e^{-\frac{h^2}{2\sigma^2}} \quad (25)$$

where σ^2 is the power parameter. Then, by applying $C_{o1}(\alpha, \omega) = 2P_s \alpha T_N H(\alpha, \omega) / N_B$, $C_{i1}(\alpha, \omega)$, which has been defined in (24), can be written as

$$\begin{aligned} C_{i1}(\alpha, \omega) &= \int_0^{+\infty} \log_2 (1 + C_{o1}(\alpha, \omega) h^2) \frac{h}{\sigma^2} e^{-\frac{h^2}{2\sigma^2}} dh \\ &= \int_0^{+\infty} -\log_2 (1 + C_{o1}(\alpha, \omega) h^2) \left(-\frac{h}{\sigma^2} e^{-\frac{h^2}{2\sigma^2}} \right) dh. \end{aligned} \quad (26)$$

By extracting the integral items as $F_1(\alpha, \omega) = -\log_2 (1 + C_{o1}(\alpha, \omega) h^2)$ and $F_2(h) = e^{-\frac{h^2}{2\sigma^2}}$, $C_{i1}(\alpha, \omega)$ can be expressed as

$$C_{i1}(\alpha, \omega) = \int_0^{+\infty} F_1(h, \alpha, \omega) F_2'(h) dh \quad (27)$$

According to the principle of integral by parts [17], $C_i(h, \alpha, \omega)$ can be further written as

$$\begin{aligned} C_{i1}(\alpha, \omega) &= F_1(h, \alpha, \omega) F_2(h) \Big|_0^{+\infty} \\ &\quad - \int_0^{+\infty} F_1'(h, \alpha, \omega) F_2(h) dh. \end{aligned} \quad (28)$$

Due to the fact that

$$F_1(0, \alpha, \omega) F_2(0) = -\log_2(1) \cdot e^0 = 0 \quad (29)$$

and

$$\begin{aligned} &\lim_{h \rightarrow +\infty} F_1(h, \alpha, \omega) F_2(h) \\ &= \lim_{h \rightarrow +\infty} \left(-\log_2 (1 + C_{o1}(\alpha, \omega) h^2) e^{-\frac{h^2}{2\sigma^2}} \right) \\ &= 0, \end{aligned} \quad (30)$$

(28) can be obtained as

$$\begin{aligned} C_{i1}(\alpha, \omega) &= - \int_0^{+\infty} \frac{2C_{o1}(\alpha, \omega) h}{\ln 2 \cdot (1 + C_{o1}(\alpha, \omega) h^2)} e^{-\frac{h^2}{2\sigma^2}} dh \\ &= - \frac{1}{\ln 2} \int_0^{+\infty} \frac{2h}{\left(\frac{1}{C_{o1}(\alpha, \omega)} + h^2 \right)} \cdot e^{-\frac{h^2}{2\sigma^2}} dh \\ &= - \frac{1}{\ln 2} \int_0^{+\infty} \frac{2\sigma^2 e^{-\frac{C_{o1}(\alpha, \omega) + h^2}{2\sigma^2}} e^{\frac{1}{2\sigma^2 C_{o1}(\alpha, \omega)} h}}{\left(\frac{1}{C_{o1}(\alpha, \omega)} + h^2 \right) \sigma^2} dh \\ &= - \frac{e^{\frac{1}{2\sigma^2 C_{o1}(\alpha, \omega)}}}{\ln 2} \int_{\frac{1}{2\sigma^2 C_{o1}(\alpha, \omega)}}^{+\infty} \frac{2\sigma^2 e^{-\frac{C_{o1}(\alpha, \omega) + h^2}{2\sigma^2}}}{\left(\frac{1}{C_{o1}(\alpha, \omega)} + h^2 \right)} \\ &\quad d\left(\frac{1}{\frac{1}{2\sigma^2} + h^2} \right) \\ &= - \frac{e^{\frac{N_B}{4\sigma^2 P_s \alpha T_N H(\alpha, \omega)}}}{\ln 2} \text{Ei} \left(-\frac{N_B}{4\sigma^2 P_s \alpha T_N H(\alpha, \omega)} \right), \end{aligned} \quad (31)$$

where $\text{Ei}(x)$ is the exponential integral function which is defined as

$$\text{Ei}(x) = \int_{-x}^{+\infty} \frac{e^{-t}}{t} dt. \quad (32)$$

Now, by applying $C_{o2}(\alpha) = -4\sigma^2 P_s \alpha T_N / N_B$, (24) can be written as

$$C_{B'}(\alpha) = -\frac{1}{\pi\alpha(1+\beta)\ln 2} \underbrace{\int_0^\pi e^{-\frac{C_{o2}(\alpha)}{H(\alpha, \omega)}} \text{Ei} \left(\frac{C_{o2}}{H(\alpha, \omega)} \right) d\omega}_{C_{i2}(\alpha, \omega)} \quad (33)$$

Then, we split $C_{i2}(\alpha, \omega)$ into several subsection integral and calculate them respectively. For $\omega \in [0, b_1(\alpha)]$, the integral can be calculated as

$$\begin{aligned} C_{R4}(\alpha) &= \int_0^{b_1(\alpha)} e^{-\frac{C_{o2}(\alpha)}{H(\alpha, \omega)}} \text{Ei}\left(\frac{C_{o2}}{H(\alpha, \omega)}\right) d\omega \\ &= \int_0^{b_1(\alpha)} e^{-\alpha C_{o2}(\alpha)} \text{Ei}(\alpha C_{o2}(\alpha)) d\omega \\ &= \alpha \pi (1 - \beta) e^{-\alpha C_{o2}} \text{Ei}(\alpha C_{o2}(\alpha)) \end{aligned} \quad (34)$$

According to the Gaussian-Chebyshev quadrature, for $\omega \in [b_1(\alpha), \pi]$, the integral can be written as

$$\begin{aligned} C_{R5}(\alpha) &= \int_{b_1(\alpha)}^{\pi} e^{-\frac{C_{o2}(\alpha)}{H(\alpha, \omega)}} \text{Ei}\left(\frac{C_{o2}}{H(\alpha, \omega)}\right) d\omega \\ &\approx C_1 \sum_{i=1}^N m_i e^{-\frac{C_{o2}(\alpha)}{H(\alpha, \omega_{1i})}} \text{Ei}\left(\frac{C_{o2}}{H(\alpha, \omega_{1i})}\right) \end{aligned} \quad (35)$$

Similarly, for $\omega \in [b_1(\alpha), b_3(\alpha)]$, the integral can be written as

$$\begin{aligned} C_{R6}(\alpha) &= \int_{b_1(\alpha)}^{b_3(\alpha)} e^{-\frac{C_{o2}(\alpha)}{H(\alpha, \omega)}} \text{Ei}\left(\frac{C_{o2}}{H(\alpha, \omega)}\right) d\omega \\ &\approx C_2 \sum_{i=1}^N m_i e^{-\frac{C_{o2}(\alpha)}{H(\alpha, \omega_{2i})}} \text{Ei}\left(\frac{C_{o2}}{H(\alpha, \omega_{2i})}\right) \end{aligned} \quad (36)$$

Finally, the capacity of the proposed scheme in Rayleigh channel can be written as

$$C_{B'}(\alpha) = \begin{cases} C_{R4}(\alpha) + C_{R5}(\alpha), & b_2(\alpha) < \pi \\ C_{R4}(\alpha) + C_{R6}(\alpha), & b_2(\alpha) \geq \pi \end{cases} \quad (37)$$

The average capacity of the proposed scheme in Rayleigh channel can be obtained as

$$C_{AB'} = \frac{1}{N_\alpha} \sum_{i=1}^{N_\alpha} C_{B'}(\alpha_i). \quad (38)$$

C. Capacity of the Alice-Bob Link in Nakagami- m Channel

The capacity of FTN signaling with packing ratio α in Nakagami- m channel can be formulated as

$$\begin{aligned} R_{B''}(\alpha) &= \frac{1}{\pi \alpha (1 + \beta)} \cdot \\ &\underbrace{\int_0^{\pi} \int_0^{+\infty} f_N(h) \cdot \log_2 \left(1 + \frac{2h^2 P_s \alpha T_N}{N_B} H(\alpha, \omega) \right) dh d\omega}_{R_{i2}(\alpha, \omega)} \end{aligned} \quad (39)$$

where $f_N(h)$ is the PDF of the channel gain h in Nakagami- m channel which can be written as

$$f_N(h) = \frac{2m^m h^{2m-1}}{\Gamma(m) P_r^m} e^{-\frac{m h^2}{P_r}} \quad (40)$$

where m ($m > 0$) is the fading parameter, P_r is the average power, $\Gamma(m)$ is the Gamma function which can be expressed as [18]

$$\Gamma(m) = \int_0^{+\infty} t^{m-1} e^{-t} dt \quad (m > 0) \quad (41)$$

By applying $C_{o3} = 2m^m / (\Gamma(m) P_r^m)$, the integral of channel gain h can be written as

$$\begin{aligned} R_{i,2}(\alpha, \omega) &= \int_0^{+\infty} C_{o3} h^{2m-1} e^{-\frac{m h^2}{P_r}} \log_2 (1 + C_{o1}(\alpha, \omega) h^2) dh \\ &= C_{o3} \mathcal{M} \left[e^{-\frac{m h^2}{P_r}} \log_2 (1 + C_{o1}(\alpha, \omega) h^2); 2m \right] \end{aligned} \quad (42)$$

where $\mathcal{M}[f(x); s]$ means the Mellin transform [19] of $f(x)$. According to the Mellin convolution theorem, (42) can be further expressed as

$$\begin{aligned} R_{i,2}(\alpha, \omega) &= \frac{C_{o3}}{2\pi i} \int_{c-i\infty}^{c+i\infty} M \left[e^{-\frac{m h^2}{P_r}}; u \right] \cdot \\ &\quad M \left[(1 + C_{o1}(\alpha, \omega) h^2); (2m - u) \right] du \\ &= \frac{C_{o3}}{2\pi i} \int_{c-i\infty}^{c+i\infty} \frac{\Gamma(m - \frac{u}{2}) \left(\frac{P_r}{m}\right)^{m - \frac{u}{2}} \pi}{2C_{o1}(\alpha, \omega) u \cdot \ln(2) \sin(\frac{\pi u}{2})} du \\ &= \frac{C_{o3}}{2 \ln 2} \left(\frac{P_r}{m}\right)^m \cdot G_{2,3}^{3,1} \left(\begin{array}{c} 0, 1 \\ 0, 0, m \end{array} \middle| \frac{m}{C_{o1}(\alpha, \omega) P_r} \right) \\ &= \frac{1}{\Gamma(m) \ln 2} \cdot G_{2,3}^{3,1} \left(\begin{array}{c} 0, 1 \\ 0, 0, m \end{array} \middle| \frac{m}{C_{o1}(\alpha, \omega) P_r} \right) \end{aligned} \quad (43)$$

where $G_{p, q}^{m, n} \left(\begin{array}{c} a_1, a_2 \dots a_p \\ b_1, b_2 \dots b_q \end{array} \middle| z \right)$ represents the Meijer-G function [20].

Similar to (34) and (35), by applying $C_{o4} = m N_B / (2P_s \alpha T_N P_r)$, for $\omega \in [0, b_1(\alpha)]$, the integral of ω can be written as

$$\begin{aligned} C_{R7}(\alpha) &= \int_0^{b_1(\alpha)} \frac{1}{\Gamma(m) \ln(2)} \cdot G_{2,3}^{3,1} \left(\begin{array}{c} 0, 1 \\ 0, 0, m \end{array} \middle| \frac{m}{C_{o1}(\alpha, \omega) P_r} \right) d\omega \\ &= \int_0^{b_1(\alpha)} \frac{1}{\Gamma(m) \ln(2)} \cdot G_{2,3}^{3,1} \left(\begin{array}{c} 0, 1 \\ 0, 0, m \end{array} \middle| \alpha C_{o4}(\alpha, \omega) \right) d\omega \\ &= \frac{\alpha \pi (1 - \beta)}{\Gamma(m) \ln(2)} \cdot G_{2,3}^{3,1} \left(\begin{array}{c} 0, 1 \\ 0, 0, m \end{array} \middle| \alpha C_{o4}(\alpha, \omega) \right) \end{aligned} \quad (44)$$

For $\omega \in [b_1(\alpha), \pi]$, the integral can be written as

$$\begin{aligned} C_{R8}(\alpha) &= \int_{b_1(\alpha)}^{\pi} \frac{1}{\Gamma(m) \ln(2)} \cdot G_{2,3}^{2,2} \left(\begin{array}{c} 1, 1 \\ m, 1, 0 \end{array} \middle| \frac{C_{o4}}{H(\alpha, \omega)} \right) d\omega \\ &\approx \frac{C_1}{\Gamma(m) \ln(2)} \sum_{i=1}^N m_i \cdot G_{2,3}^{2,2} \left(\begin{array}{c} 1, 1 \\ m, 1, 0 \end{array} \middle| \frac{C_{o4}}{H(\alpha, \omega_{1i})} \right) \end{aligned} \quad (45)$$

And for $\omega \in [b_1(\alpha), b_3(\alpha)]$, the integral can be written as

$$\begin{aligned} C_{R9}(\alpha) &= \int_{b_1(\alpha)}^{b_3(\alpha)} \frac{1}{\Gamma(m) \ln(2)} \cdot G_{2,3}^{2,2} \left(\begin{array}{c} 1, 1 \\ m, 1, 0 \end{array} \middle| \frac{C_{o4}}{H(\alpha, \omega)} \right) d\omega \\ &\approx \frac{C_2}{\Gamma(m) \ln(2)} \sum_{i=1}^N m_i \cdot G_{2,3}^{2,2} \left(\begin{array}{c} 1, 1 \\ m, 1, 0 \end{array} \middle| \frac{C_{o4}}{H(\alpha, \omega_{2i})} \right) \end{aligned} \quad (46)$$

Finally, the capacity of the proposed scheme in Nakagami channel can be written as

$$C_{B''}(\alpha) = \begin{cases} C_{R7}(\alpha) + C_{R8}(\alpha), & b_2(\alpha) < \pi \\ C_{R7}(\alpha) + C_{R9}(\alpha), & b_2(\alpha) \geq \pi \end{cases}. \quad (47)$$

And the average capacity of the proposed scheme in Nakagami channel can be written as

$$C_{AB''} = \frac{1}{N_\alpha} \sum_{i=1}^{N_\alpha} C_{B''}(\alpha_i). \quad (48)$$

D. Analysis of Alice-Eve Link

Due to the knowledge absence of the starting position and corresponding α value, Eve cannot estimate α exactly nor employ the correct sampling rate. When Eve employs a wrong α value, the symbols he samples will quickly deviate their right positions. For example, if Alice and Eve employs 0.9 and 0.75 as their symbol packing ratio respectively, Eve's 20-th sampled position is near to the 17-th transmitted symbol and contains nearly no available information of the 20th transmitted symbol. So, the degradation in BER performance for Eve is obvious. In this paper, We employ the assumption that Eve use a fixed-value α for the whole transmission process. And when $\alpha_E = \alpha_A$, the sampling offset is not taken into consideration.

Different from other physical layer paradigms, the proposed transmission system does not directly change the signal-to-interference-noise ratio (SINR). So, we use bit error rate (BER) performance rather than spectrum efficiency or transmission rate to evaluate the ability of Eve to recover the transmitted symbols, which will be shown in Section V.

V. NUMERICAL RESULTS

In this section, we carry out the comprehensive analysis and evaluation of the proposed safe and high-speed transmission system. In this paper, we employ the square root raised cosine (SRRC) filter as the shaping and matching filters. And the training parameters for the DNN in the proposed simplified symbol packing ratio estimation are listed in Table I.

TABLE I. Training and testing parameters of the DNN in the proposed simplified symbol packing ratio estimation

item	value
number of neurons	(20, 1000, 500, 250, 1)
training data size	3×10^6 groups
training E_b/N_0	4dB
training epoch	50
optimizer	Adam
loss function	mean square error (MSE)
learning rate	0.001
start / end sparsity	0 / 0.5
testing data size	3×10^6 groups

A. Spectrum Efficiency of the Proposed Communication Scheme in AWGN Channel

The average spectrum efficiencies of the proposed scheme in AWGN channel are illustrated in Fig. 5 and Fig. 6 with

roll-off factor $\beta = 0.5$ and $\beta = 0.3$ respectively. the curve labeled *Monte-Carlo* is obtained by independent repeated trials with randomly generated channel gain h values. And the curve labeled *theoretical* is calculated by (21). The perfect match of the results by theoretical derivation and the Monte-Carlo simulation proves the correctness of the SE obtained in Section IV.

Also, as can be seen from the figures, by employing FTN signaling with different α values, the proposed system can achieve up to 20% higher average spectrum efficiency gain beyond conventional Nyquist-criterion systems, without any extra spectrum resources required. It can obviously improve the utilization of the precious spectrum resources and meet the requirement of the increasing demand from communication business on the data traffic.

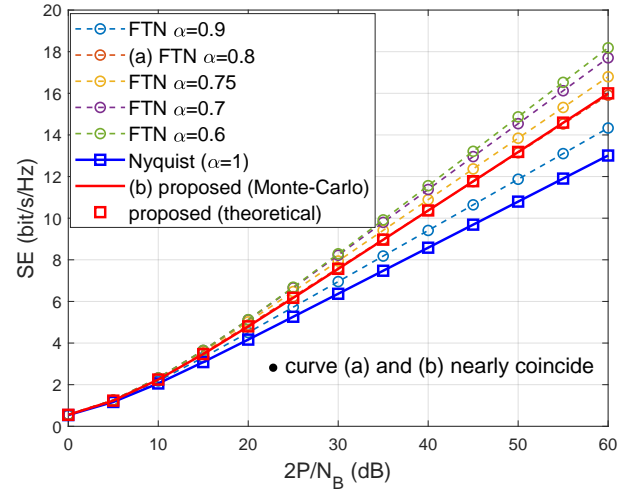


Fig. 5. The spectrum efficiency of the proposed high-spectrum-efficiency and safe transmission system

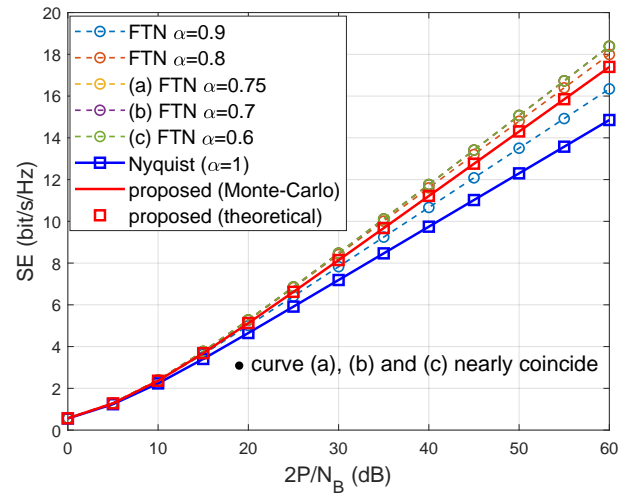


Fig. 6. The spectrum efficiency of the proposed high-spectrum-efficiency and safe transmission system

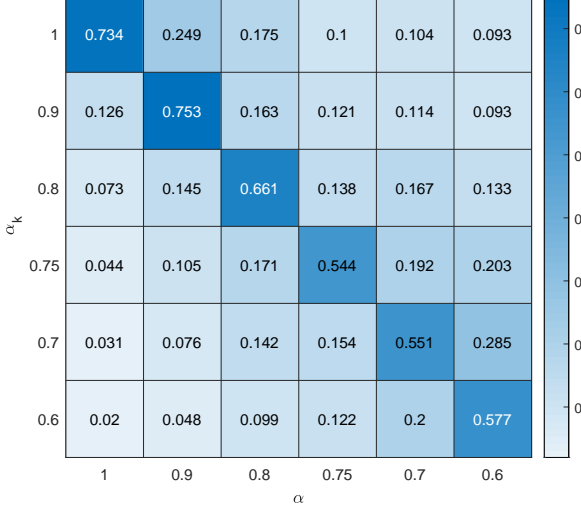


Fig. 7. The comparison of the proposed simplified estimation and its original structure in the minimum times of decisions required to achieve a 99% accuracy

B. Performance of the Proposed Estimation for FTN Signaling in AWGN Channel

Although the spectrum efficiency gain of the proposed scheme has been proved by the analysis and the simulation, an effective blind estimation for packing ratio is required to make the communications available. Fig. 7 illustrates the accuracy performance of the proposed packing ratio estimation in AWGN under $\text{SNR} = 4\text{dB}$. α is the true packing ratio of the input data. Every grid represents the probability to output 1 when the estimation for whether $\alpha = \alpha_k$ is implemented. The estimations for all α values are carried out independently and the α_k with the most 1 output is considered as the true packing ratio of the data. Hence, the sum value of any row or column in Fig. 7 does not have to be 1.

As can be seen from the figure, for the data with any true packing ratio value α , the estimation for $\alpha_k = \alpha$ always outputs the most 1 values so that the system can choose the correct α_k as the estimated packing ratio value. This has proved the effectiveness of the proposed simplified estimation algorithm.

C. Spectrum Efficiency of the Proposed Communication Scheme in Rayleigh and Nakagami Channels

Fig. 8 and Fig. 9 illustrates the average spectrum efficiency of the proposed transmission scheme in Rayleigh and Nakagami channels. Similar to that in AWGN channel, the spectrum efficiency of the proposed scheme in such two scenarios outperforms the conventional Nyquist transmission. This means a higher data rate is achievable in more practical channels without any extra spectrum resources by employing the transmission scheme proposed in this paper.

Also, as can be seen, the Monte-Carlo simulation fits the curve with theoretical data provided in Section IV. It shows that (38) and (48) accurately describe the actual capacities of the proposed scheme in Rayleigh and Nakagami channels.

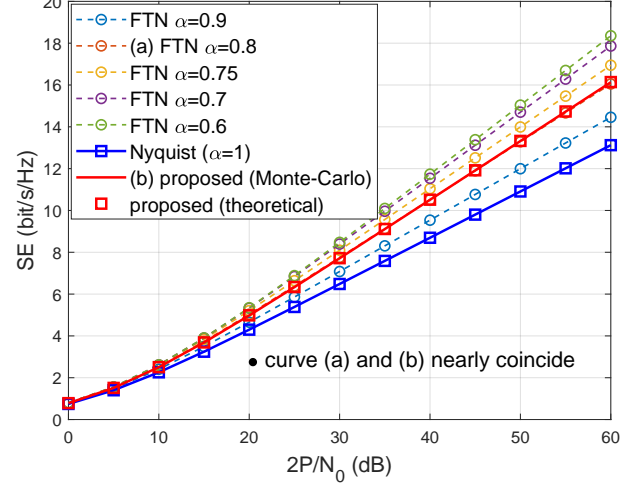


Fig. 8. The spectrum efficiency of the proposed high-spectrum-efficiency and safe transmission system

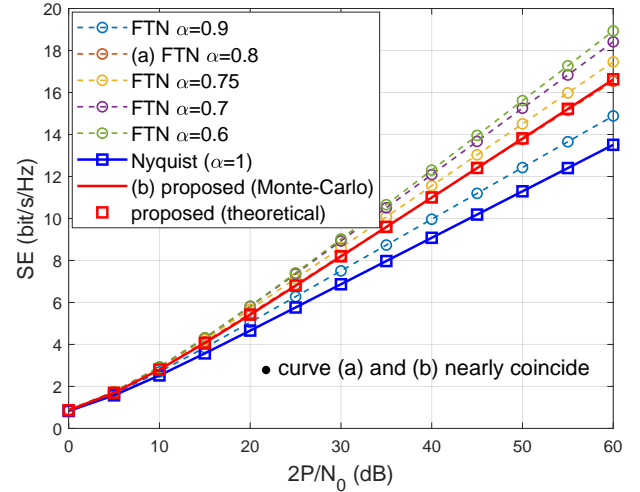


Fig. 9. The spectrum efficiency of the proposed high-spectrum-efficiency and safe transmission system

D. Performance of the Proposed Estimation for FTN Signaling in Rayleigh and Nakagami Channels

Fig. 10 and Fig. 11 illustrates the estimation accuracy for different α and α_k values in Rayleigh ($\text{SNR}=25\text{dB}$) and Nakagami ($\text{SNR}=18\text{dB}$) channels respectively. Similar to Fig. 7, the value of each grid represents the probability to output 1 when the estimation for whether $\alpha = \alpha_k$ is carried out.

As can be seen from the figures, the true decision for each α value always corresponds to the biggest probability to output 1. This means that after a certain time to count the number of 1 in each branch, the system will finally choose the right α_k to be the estimated α values. Hence, the simplified estimation for α is proved to be effective.

E. BER Performance of Alice-Bob and Alice-Eve Link

In this part, we provide the BER performance of the proposed transmission system, as shown in Fig. 12. In Alice-Bob and Alice-Eve link, maximum a priori probability (MAP)

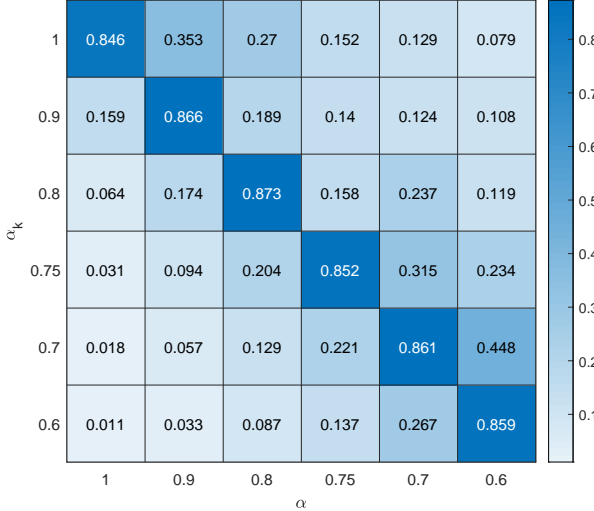


Fig. 10. The comparison of the proposed simplified estimation and its original structure in the minimum times of decisions required to achieve a 99% accuracy

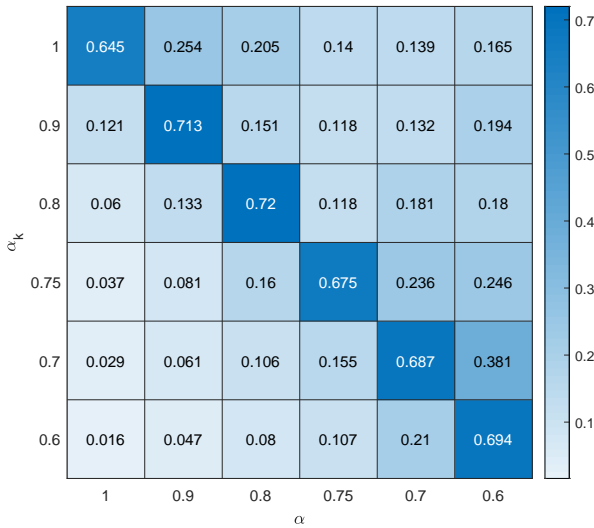


Fig. 11. The comparison of the proposed simplified estimation and its original structure in the minimum times of decisions required to achieve a 99% accuracy

[21] is employed as the detection algorithm. And the BER in Nyquist-criterion system, which is shown in *AWGN bound*, is also presented for comparison.

As can be seen, Bob can achieve nearly the same BER performance as that in the ISI-free AWGN channel. For Eve, when $\alpha_E \neq \alpha_A$, he will neither be able to sample the received signals by the expected interval nor recovery the transmitted symbols. Although we assume that when $\alpha_E = \alpha_A$, Eve can sample the received signal at the accurate position without any sampling offset, the average BER of Alice-Eve link, as shown, is still poor enough. This result effectively proves the security of our proposed transmission.

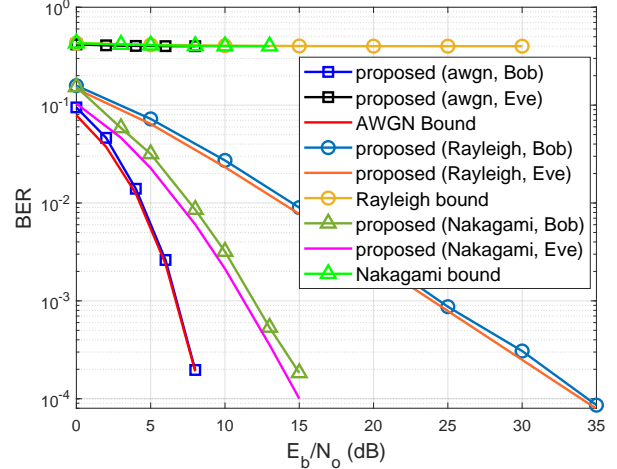


Fig. 12. BER performance of the proposed system for Alice-Bob and Alice-Eve links versus conventional Nyquist-criterion transmission

F. Complexity and Performance of the Proposed Simplified Symbol Packing Ratio Estimation

For the convenience of representation, we just provide the complexity of the analysis for $\alpha = 0.7$, while the total complexity is approximately proportional to this result. Table II provides the complexity of the proposed simplified symbol ratio estimation compared to its original structure [14].

As shown, the proposed structure nearly removes all the MUX, DEMUX, sum, maximum and S/P operations in the original structure. Also, in the sparse DNN employed in our proposed simplified estimation, the number of items in each layer has been reduced to half of that in the original network. Especially, benefiting from both the sparse DNN and the single branch, the number of multiply-add operations required for each estimation has been reduced to 5% of that in the original architecture. This allows more flexibility for researchers to balance the resource of time and space in practical implementation.

To more visually show the performance of the proposed simplified estimation, we employ the accuracy of the estimation as [14]

$$P_{\text{acc}} = \sum_{m=1}^M \sum_{n=0}^{m-1} \left(C_M^m C_M^n (p_1)^m (1-p_1)^{(M-m)} \cdot (p_2)^n (1-p_2)^{(M-n)} \right) \quad (49)$$

where M is the number of decisions used for the selection of the maximum one. p_1 is the probability that the analysis for $\alpha_k = \alpha$ gives the true decision. And p_2 is the maximum one of the probabilities that the analysis for $\alpha_k \neq \alpha$ produces the true decision.

Fig. 13 shows the minimum number of decisions required to achieve a 99% accuracy ($P_{\text{acc}} > 0.99$). As seen, the proposed simplified estimation can converge nearly as fast as the original structure within 35 estimation times, although the complexity has been greatly reduced.

TABLE II. The complexity comparison between the proposed simplified estimation and its original structure

Algorithm	MUX	DEMUX	sum	max	S/P	$\ \mathbf{W}_1\ _0$	$\ \mathbf{W}_2\ _0$	$\ \mathbf{W}_3\ _0$	$\ \mathbf{W}_4\ _0$	Multi-Add per estimation
Original Structure	1	2	10	1	10	20K	500K	125K	0.25K	645.25K
Proposed Structure	0	0	1	0	1	10K	125K	62.5K	0.125K	about 32.263K

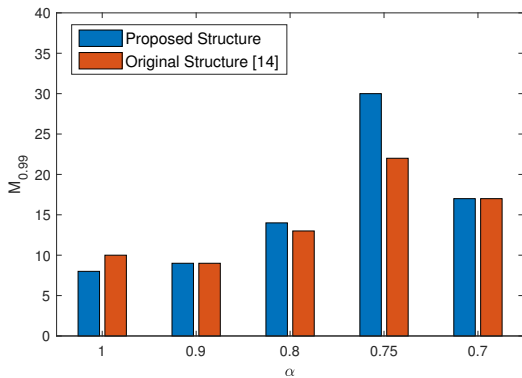


Fig. 13. The comparison of the proposed simplified estimation and its original structure in the minimum times of decisions required to achieve a 99% accuracy

G. The Robustness of the Simplified Estimation to SNR values

Here, we take AWGN channel as an example. The performance of the proposed simplified estimation in different SNR values is listed in Table III. As shown, although the model is trained at $E_b/N_0=4$ dB, it can work well for the scenarios with other SNR values. It can effectively reduce the complexity of the training process and the practical implementation for our proposed estimation.

TABLE III. Performance of the proposed estimation (trained at $E_b/N_0=4$ dB) for different SNR values

E_b/N_0	P_{true} for $\alpha_k = \alpha$	Maximum P_{true} for $\alpha_k \neq \alpha$
4dB	0.7876	0.2063
3dB	0.5084	0.1596
2dB	0.4372	0.1463
1dB	0.2914	0.1485

VI. CONCLUSION

In this paper, we propose a secure transmission system with high spectrum efficiency based on FTN and DL. The transmitter changes its symbol packing ratio α to a new random value at every specific moment. By the shared information of starting positions, the receiver can estimate the current α and then detect the FTN signal, while the eavesdropper can not due to the absence of required knowledge. Numerical results show that the proposed system can achieve a secure and higher-spectrum-efficiency communication without the consumption of any extra spectrum resources. Also, a simplified symbol packing ratio, which has been employed in the proposed system, is developed in this paper. Simulation results prove that it achieves nearly the same performance as the original structure with only 5% of the original complexity.

ACKNOWLEDGMENT

This work is supported in part by the National Key R&D Program of China (2018YFE0100500), the National Natural Science Foundation of Shaanxi Province (2019CGXNG-010, 2020CGXNG-036, 2019JQ-658), China's Postdoctoral Grants (2018M640958) and Youth Program of National Natural Science Foundation of China (61901325).

REFERENCES

- [1] Q. Li, F.-K. Gong, P. Song, and S. Zhai, "Beyond DVB-S2X: Faster-than-Nyquist signaling with linear precoding," *IEEE Trans. Broadcast.*, to be published, 2018, DOI:10.1109/TBC.2019.2960941.
- [2] J. E. Mazo, "Faster-than-Nyquist signaling," *Bell System Technical Journal*, vol. 54, no. 8, pp. 1451–1462, 1975.
- [3] A. D. Liveris and C. N. Georghiades, "Exploiting faster-than-Nyquist signaling," *IEEE Trans. Commun.*, vol. 51, no. 9, pp. 1502–1511, 2003.
- [4] J. B. Anderson, A. Prlja, and F. Rusek, "New reduced state space BCJR algorithms for the ISI channel," in *Proc. IEEE Int. Symp. Information Theory*, Seoul, South Korea. IEEE, 2009, pp. 889–893.
- [5] E. Bedeer, M. H. Ahmed, and H. Yanikomeroglu, "A very low complexity successive symbol-by-symbol sequence estimator for faster-than-Nyquist signaling," *IEEE Access*, vol. 5, no. 99, pp. 7414–7422, 2017.
- [6] P. Song, F. Gong, Q. Li, G. Li, and H. Ding, "Receiver design for faster-than-Nyquist signaling: Deep-learning-based architectures," *IEEE Access*, vol. 8, pp. 68 866–68 873, 2020.
- [7] S. Sugiura, "Frequency-domain equalization of faster-than-Nyquist signaling," *IEEE Wireless Commun. Lett.*, vol. 2, no. 5, pp. 555–558, 2013.
- [8] T. Ishihara and S. Sugiura, "Frequency-domain equalization aided iterative detection of faster-than-Nyquist signaling with noise whitening," in *Proc. IEEE Int. Conf. Commun. (ICC)*, Kuala Lumpur, Malaysia. IEEE, 2016, pp. 1–6.
- [9] J. Wang, W. Tang, X. Li, and S. Li, "Filter hopping based faster-than-Nyquist signaling for physical layer security," *IEEE Wireless Commun. Lett.*, vol. 64, no. 5, pp. 2122–2128, 2018.
- [10] H. Ye, G. Y. Li, and B.-H. Juang, "Power of deep learning for channel estimation and signal detection in OFDM systems," *IEEE Wireless Commun. Lett.*, vol. 7, no. 1, pp. 114–117, 2018.
- [11] E. Balevi and J. G. Andrews, "One-bit OFDM receivers via deep learning," *IEEE Trans. Commun.*, 2019.
- [12] Y. Su, X. Lu, Y. Zhao, L. Huang, and X. Du, "Cooperative communications with relay selection based on deep reinforcement learning in wireless sensor networks," *IEEE Sensors J.*, vol. 19, no. 20, pp. 9561–9569, 2019.
- [13] K. K. Nguyen, T. Q. Duong, N. A. Vien, N.-A. Le-Khac, and M.-N. Nguyen, "Non-cooperative energy efficient power allocation game in D2D communication: A multi-agent deep reinforcement learning approach," *IEEE Access*, vol. 7, pp. 100 480–100 490, 2019.
- [14] P. Song, F. Gong, and Q. Li, "Blind symbol packing ratio estimation for faster-than-nyquist signalling based on deep learning," *Electron. Lett.*, vol. 55, no. 21, pp. 1155–1157, 2019.
- [15] F. Rusek and J. B. Anderson, "Constrained capacities for faster-than-Nyquist signaling," *IEEE Trans. Inf. Theory*, vol. 55, no. 2, pp. 764–775, 2009.
- [16] I. S. Gradshteyn and I. M. Ryzhik, *Table of integrals, series, and products*. Academic press, 2014.
- [17] G. B. Thomas and R. L. Finney, *Calculus*. Addison-Wesley Publishing Company, 1961.
- [18] C. C. Ross, *Differential equations: an introduction with Mathematica®*. Springer Science & Business Media, 2004.
- [19] P. Flajolet, X. Gourdon, and P. Dumas, "Mellin transforms and asymptotics: Harmonic sums," *Theoretical computer science*, vol. 144, no. 1-2, pp. 3–58, 1995.
- [20] H. Bateman, *Higher transcendental functions [volumes i-iii]*. McGraw-Hill Book Company, 1953, vol. 1.

[21] S. Li, B. Bai, J. Zhou, P. Chen, and Z. Yu, “Reduced-complexity equalization for faster-than-Nyquist signaling: New methods based on Ungerboeck observation model,” *IEEE Trans. Commun.*, vol. 66, no. 3, pp. 1190–1204, 2018.